

New experimental techniques for validation of marine discharge models

Philip J.W. Roberts ^{*}, Xiaodong Tian

School of Civil and Environmental Engineering, Georgia Institute of Technology, Atlanta, GA 30332, USA

Received 11 March 2002; received in revised form 24 May 2002; accepted 8 August 2003

Abstract

A new three-dimensional Laser-Induced Fluorescence (3DLIF) system was applied to study the mixing of a produced water outfall discharge typical of that used in offshore production operations. The outfall consists of a pipeline terminating in a multiport diffuser discharging into water about 12 m deep. Scaled laboratory experiments were done using conditions based on measured oceanographic conditions near the site. The current was perpendicular to the diffuser, and the receiving water was linearly stratified. The model was undistorted and the jet densimetric Froude number was the same as in the prototype. This scaling results in correct modeling of the source volume, momentum, and buoyancy fluxes, and equality of other line source dimensionless parameters. The experiments were conducted in a constant refractive-index environment which enabled detailed three-dimensional concentration measurements in the near field mixing zone to be obtained despite the density variations in the flow field. The mixing processes were found to be complex. The jets discharging upstream were quickly swept downstream, where they began merging with the downstream jets. Lateral mixing caused the concentration profiles to quickly become laterally homogeneous. Initially, dilution increased rapidly with distance from the diffuser, but farther away the rate of increase of dilution slowed as the turbulence became affected by the ambient density stratification. The dilution eventually becomes approximately constant; the location where this occurs defines the end of the near field, where mixing is primarily due to turbulence and other processes induced by the discharge itself. The end of the near field is marked by collapse of the self-induced turbulence under the influence of the ambient stratification.

The results were compared to predictions of commonly used mathematical models of marine mixing zones: RSB, UM3, and CORMIX. The best predictions of the near field dilution and the length of the near field were by RSB. UM3 gave good predictions of the near field dilution, but CORMIX overestimated the dilution and rise height substantially. It is believed that this overestimation by CORMIX is due to its approximation of the diffuser as a row of vertically discharging jets of equivalent total momentum flux; this is clearly a poor approximation to the diffuser conditions modeled here.

3DLIF is an exciting new technique that can give unprecedented insight into the complex hydrodynamics and processes occurring in buoyancy-modified mixing zones and to improvement of near field mathematical models. Experiments on other discharge configurations are continuing.

© 2003 Elsevier Ltd. All rights reserved.

Keywords: Mixing zones; Mathematical models; Dilution; Dispersion; Ocean outfalls

1. Introduction

Modeling the characteristics of mixing zones for waste water discharges into a marine environment is a difficult task. For example, produced water (water extracted along with oil or gas in the production process)

is often discharged back into the ocean through a submarine outfall. The outfall may include a diffuser with many ports from which the waste water is discharged as high velocity jets. Depending on local conditions, the produced water may be more or less dense than sea water. If less dense, buoyancy forces cause the jets to ascend towards the water surface. The velocity shear between the buoyant jets and their surroundings causes turbulence which entrains external sea water and mixes with it, resulting in rapid mixing. Further complications arise due to the effects of ambient currents and oceanic

^{*} Corresponding author. Tel.: +1-404-894-2219; fax: +1-404-385-1131.

E-mail address: proberts@ce.gatech.edu (P.J.W. Roberts).

density stratification. Currents sweep the jets downstream, increasing dilution; stratification can trap the rising plumes below the water surface, reducing dilution. Yet more complications arise from merging of the individual jets. Close to the source, mixing is dominated by turbulence which is generated by the discharge itself. The region in which this occurs is known as the near field. This self-induced turbulence decays with distance from the source, and mixing due to ambient oceanic turbulence becomes increasingly important; the region in which mixing is primarily due to ambient turbulence is known as the far field. For further discussions of mixing zones, see [Jirka and Akar \(1991\)](#); [Roberts \(1999\)](#), and others.

Mathematical models are often used to predict the behavior of the discharge in the near field. Well-known examples of models, available from the US EPA, are UM3 (in Visual PLUMES), RSB, and CORMIX, which will be discussed further below. Detailed verification of near field models is lacking, however. Field measurements of operating outfalls are difficult, particularly with submerged plumes, and the corresponding environmental conditions, such as currents and density stratification, are rarely well known.

Controlled experiments in the laboratory overcome some of these deficiencies, but have drawbacks of their own. It is difficult to simulate a flowing stratified environment in the laboratory, particularly at scales large enough to ensure reasonable similitude, and that make the jet Reynolds number high enough to result in turbulent flow. Measurements of dilution, which is usually the main objective, have also been limited. Typically, the concentration of some scalar tracer is measured in samples extracted from the flow. Examples include fluorescent dyes measured with a fluorometer ([Isaacson et al., 1983](#); [Wong and Wright, 1988](#)), and dye concentration measured by light absorption ([Roberts and Snyder, 1993](#)). This process is cumbersome and may require introduction of a sampling rack that disturbs the flow. Furthermore, the number of points sampled is limited to about 100, and only time-averaged concentrations can be measured, yielding no information on turbulent fluctuations.

More recently, Laser Induced Fluorescence (LIF) has become widely used. This is attractive as it is non-intrusive and can measure instantaneous scalar concentrations at thousands of points simultaneously. Although LIF has been extensively used in *unstratified* environments, its use in *stratified* environments has been limited by refractive index fluctuations caused by density differences. These limitations are particularly severe in large facilities because the long distance that the laser must traverse through the fluid, combined with internal waves, can cause significant laser intensity variations. These difficulties can be overcome by the use of refractive index matching (RIM) in which liquids of different density,

but equal refractive index are used. RIM in stratified flows was first suggested by [McDougall \(1979\)](#) and has since been used by many others, including [Daviero et al. \(2001\)](#). Most LIF applications have been limited to two dimensional observations, i.e. measurements in a plane.

Three-dimensional LIF (3DLIF) systems have recently become feasible thanks to rapid technological advances in computers, high speed video imaging sensors, image processing, and mass storage. These systems, in combination with refractive index matching, are capable of measuring concentration distributions in three dimensions in flowing and stationary, and stratified and unstratified environments. Such a system is described in [Tian and Roberts \(2001\)](#). These systems have the promise of yielding great advances in understanding complex mixing processes, and improving mathematical models of mixing zones.

The purpose of this paper is to illustrate the application of a 3DLIF system to measure the mixing characteristics of produced water discharged from a marine outfall under typical oceanic conditions. Scale model tests are reported and the characteristics of near field mixing are discussed. The results are then compared to predictions of commonly used mathematical models, and the limitations of the models are discussed.

2. Produced water outfall

The produced water outfall chosen to demonstrate the technique is located in the Santa Barbara Channel near Carpinteria, California ([Fig. 1](#)). Although this outfall is no longer discharging, it is still representative of a typical produced water outfall. For details of this outfall, see [Washburn et al. \(1999\)](#).

The outfall consists of a pipeline about 300 m long laid along the seabed terminating in a multiport diffuser. The mean water depth at the diffuser is about 12 m. The diffuser consists of seven Tee-shaped risers, each containing two opposed ports 29.5 mm in diameter that discharge horizontally in a direction perpendicular to the diffuser axis. The risers are spaced 3.5 m apart so the total diffuser length is 21 m. The ports are one meter above the seabed. The density of the produced water is 1011.5 kg/m^3 ; it is therefore buoyant in the sea water, whose density ranges from 1023 to 1024 kg/m^3 . The average daily flowrate is $0.0306 \text{ m}^3/\text{s}$. The diffuser is oriented approximately perpendicular to the local bathymetry (and therefore to the predominant currents, see below).

Extensive oceanographic measurements made in the vicinity of the diffuser are reported in [Washburn et al. \(1999\)](#). Currents are highly variable, with speeds ranging from zero to 0.47 m/s , although speeds are less than 0.1 m/s for 90% of the time. The average current speed is

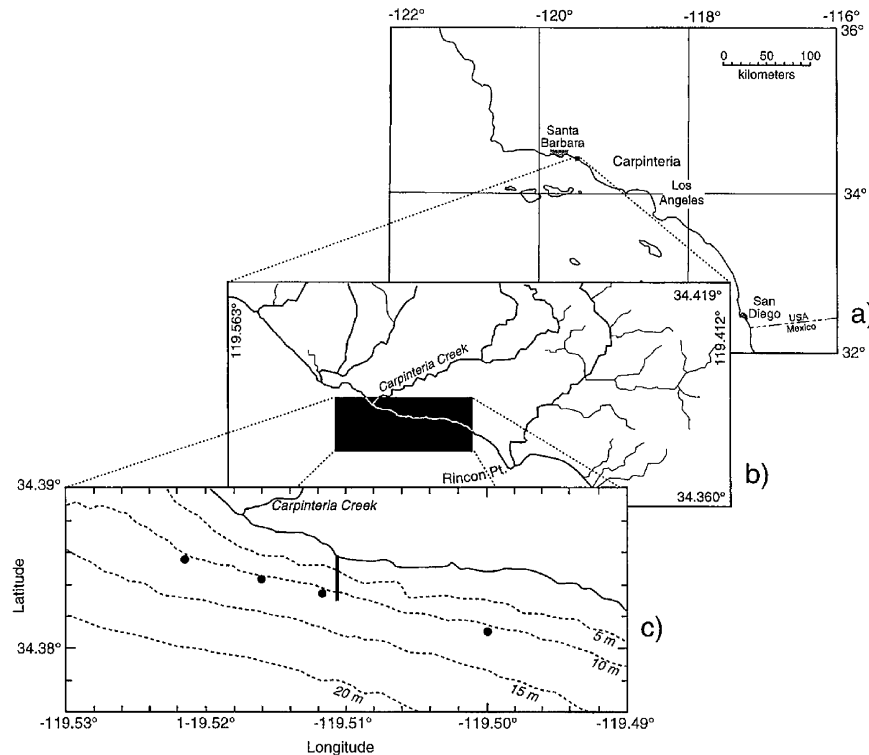


Fig. 1. (a) Area map showing outfall site near Carpinteria, CA. (b) Coastline. (c) Bathymetry (from Washburn et al., 1999).

about 0.05 m/s. The current directions are predominantly parallel to the depth contours, i.e. along-isobath, although other directions can occur. The currents are influenced by the semidiurnal (M2) tide, although low frequency currents occur in which currents can be fairly steady for several days.

Plume behavior is strongly influenced by density stratification. If strong enough, it can trap the plume below the water surface and limit the near field dilution. At this discharge site, the stratification varies seasonally. During summer, strong thermal stratification exists; during winter the stratification is weaker, and the water column can sometimes be homogeneous. Observed density differences over the water column ranged from zero to about 0.8 kg/m³. Washburn et al. (1999) report plume simulations using the mathematical model RSB which indicate that the plume is often influenced by density stratification resulting in frequent plume submergence.

Based on these observations, a typical set of conditions was chosen for the physical model. The current speed was 0.05 m/s flowing perpendicular to the diffuser. The density stratification profile was linear, with the sea water density increasing linearly from 1023.1 kg/m³ at the water surface to 1024.0 kg/m³ at the port depth of 11 m. This density difference is at the upper end of the range observed, and is chosen as a 'worst case' scenario that minimizes dilution. The test conditions are summarized in Table 1.

3. Experiments

The scale model experiments were performed in the Environmental Fluid Mechanics Laboratory at the Georgia Institute of Technology. A newly developed three-dimensional Laser Induced Fluorescence system (3DLIF) was used to measure the spatial evolution of the mixing processes induced by the diffuser and the spatial variation of dilution.

The experiments were conducted in a towing tank using the configuration shown in Fig. 2. The tank is glass-walled 6.10 m long by 0.91 m wide by 0.61 m deep and is housed in a specially built dark room. For experimental convenience, the model diffuser is inverted with a heavy discharge that falls downwards. (This is the same configuration used in Roberts and Snyder (1993) and many similar studies. It is allowable because density differences in the flow field are small compared to absolute densities: the Boussinesq assumption.) All images and results shown here are inverted to represent the actual situation, which is a positively buoyant discharge ascending upwards.

The 3DLIF system is described in Roberts and Tian (2000). It consists of two fast scanning mirrors that sweep the beam from an argon-ion laser through the flow in a programmed pattern. The system is controlled by two computers, one for timing control and synchronization, and one for image capture. A small amount of

Table 1
Summary of modeled conditions for model and prototype

	Prototype	Model
Total flow rate, Q_T (m ³ /s)	3.06×10^{-2}	1.19×10^{-5}
Port diameter, d (mm)	29.5	0.97
Riser spacing, s (m)	3.5	0.11
Number of risers, n	7	7
Diffuser length, L (m)	21	0.69
Port depth, H (m)	11.0	0.36
Jet velocity, u_j (m/s)	3.2	1.16
Current speed, u_a (m/s)	0.050	0.018
Effluent density, ρ_o (kg/m ³)	1011.5	1049.2
Ambient density at port, ρ_a (kg/m ³)	1024.0	999.2
Density difference over water column, $\Delta\rho_a$ (kg/m ³)	0.88	3.5
Jet Reynolds number, Re	94,000	1160
Jet Froude number, F_j		53
Line diffuser Froude number, F		0.70

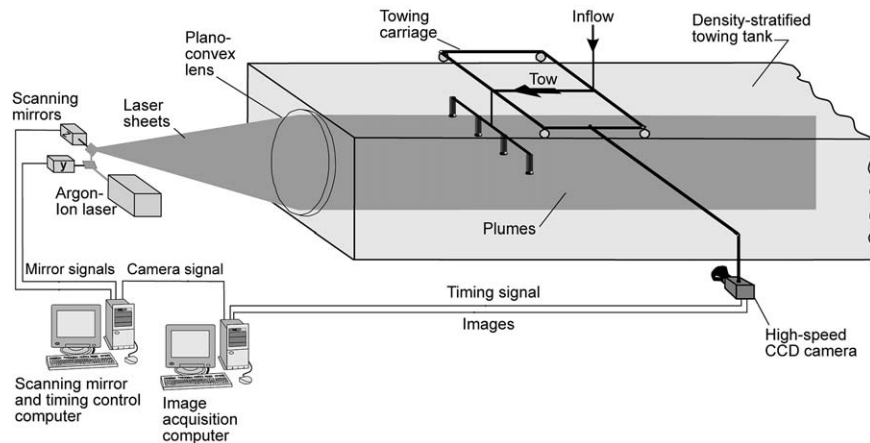


Fig. 2. Schematic depiction of experimental arrangement.

a fluorescent dye, Rhodamine 6G, is added to the effluent. The laser causes the dye to fluoresce, and the emitted light is captured by a CCD (charge-coupled device) camera. In operation, the vertical mirror sweeps the beam down and back while the camera is exposing (i.e. the shutter is 'open'). The horizontal mirror then moves the beam a small distance horizontally, the previous frame is downloaded, the camera buffer cleared, and the next exposure begun. This is repeated so that multiple vertical 'slices' through the flow are obtained. After a predetermined number of slices the beam returns to the starting point and the cycle starts again. The images are written to hard disc in real time and saved for further processing. The CCD camera resolution (number of active pixels) is 530 by 515, and the output has a resolution of 8-bits. The images are converted to quantitative scalar dye concentrations by calibration. This process involves correcting the images, pixel by pixel, for sensor response, lens luminance variation (vignetting), and laser attenuation as it passes through the tank. The procedure is described in Daviero et al. (2001). The accuracy of

the measurements thus obtained is estimated to be about $\pm 10\%$. Finally, the multiple slices through the flow are regenerated, using image processing techniques, into three-dimensional visualizations of the tracer concentration field.

The model is based on equality of the jet densimetric Froude number between model and prototype. The jet densimetric Froude number is defined as:

$$F_j = \frac{u_j}{\sqrt{g \frac{\Delta\rho}{\rho_o} d}} \quad (1)$$

where u_j is the jet velocity, g the acceleration due to gravity, $\Delta\rho$ the density difference between the effluent and receiving water, ρ_o the effluent density, and d the nozzle diameter. The jet densimetric Froude number is equal between the model and prototype and the model is undistorted. Using subscripts m to denote the model, p the prototype (i.e. the full scale outfall), and r the ratio of prototype-to-model, we have, therefore:

$$F_{jm} = F_{jp} \quad (2)$$

The length-scale ratio, $d_r = d_p/d_m$, and the model is undistorted so that all lengths are scaled in the same ratio. For example, the ratio of the spacing between the risers, s_p/s_m , and the ratio of water depths, H_p/H_m are also equal to d_r .

All other ratios are then determined uniquely by the density difference ratio $(\Delta\rho/\rho_o)_r$ and the length-scale ratio, d_r . For example, the ratios of the jet exit velocity and the ambient current speed are given by:

$$u_{jr} = u_{ar} = \left[\left(\frac{\Delta\rho}{\rho_o} \right)_r d_r \right]^{1/2} \quad (3)$$

where u_a is the ambient current speed. The ambient density profile is scaled according to:

$$\left(\frac{\rho_a(z) - \rho_a(0)}{\rho_a(0)} \right)_r = \left(\frac{\Delta\rho}{\rho_o} \right)_r \quad (4)$$

where $\rho_a(z)$ is the ambient density at height z . For further discussion of this scaling, see Roberts and Snyder (1993).

This scaling also ensures equality of other ratios. For example, an important dimensionless parameter for line diffusers is another Froude number (Roberts, 1979):

$$F = \frac{u_a^3}{b} \quad (5)$$

where $b = g(\Delta\rho/\rho_o)(Q_T/L)$ is the buoyancy flux per unit diffuser length, Q_T is the total effluent flowrate, and L the diffuser length. This Froude number is also the same in model and prototype, and the source volume, momentum, and buoyancy fluxes are correctly modeled.

The effects of molecular viscosity are not correctly modeled, however. These are characterized by the jet Reynolds number, Re :

$$Re = \frac{u_j d}{\nu} \quad (6)$$

where ν is the kinematic viscosity of the jet fluid. The Reynolds number in the model is much smaller than in the prototype. This is not a serious limitation, because, as long as the model Reynolds number is high enough that the jet quickly becomes turbulent after leaving the nozzle, the results are insensitive to the value of the Reynolds number. See Roberts and Snyder (1993) for further discussion.

The diameter of the model jets $d_m = 0.97$ mm, so the model scale $d_r = d_p/d_m = 30.5$. It is not necessary to maintain the same density difference between model and prototype. The density difference ratio $(\Delta\rho/\rho)_r$ was chosen to be 0.25, i.e. density differences in the model were four times larger than in the prototype. The advantage of this is that it increases the value of the model jet Reynolds number causing the jets to become turbulent

more quickly. The whole diffuser length (seven risers) was modeled.

The prototype and model parameter values are summarized in Table 1, including the values of the important dimensionless parameters, F_j and F . The jet Froude number $F_j = 53$. This is higher than typical for marine domestic sewage outfalls. This is because domestic sewage has a density close to that of fresh water, around 998 kg/m³. A high jet Froude number signifies that source momentum flux is likely to play a significant role in the initial mixing of the produced water, whereas it is usually unimportant for domestic sewage discharges. The significance of the line Froude number F is discussed in Roberts (1979) and Roberts et al. (1989). It determines the importance of the current speed relative to the buoyancy of the source. For the present case, the value $F = 0.7$, suggest that the plume dynamics and mixing will be significantly affected by the current.

4. Experimental procedure

The tank was filled and stratified with refractive index matched fluids (salt and ethanol) using the methods of Daviero et al. (2001). The density profile was measured by extracting water samples at various depths and measuring their densities to an accuracy of 0.1 kg/m³ with a Troemner specific gravity balance. The discharge was begun, and, after allowing time for the flow to establish, the laser scanner and the carriage movement were started. Forty images spaced approximately 3 mm apart were recorded for each sequence. The sampling area encompasses the three middle risers, extending just beyond the outer two. In prototype dimensions the sampling volume is about 7 m wide and extends from 3 m upstream of the diffuser to 17 m downstream. The images were acquired at a rate of 100 frames per second, so the sampling rate for one full sequence is 2.5 Hz.

The images were recorded for 45 s during which about 1 GB of data was captured. Images were then obtained of a calibration vessel placed in the tank containing known dye concentrations. These were used to calibrate the camera's pixel response to the dye fluorescence and to convert the images obtained in the experiments to dye concentration. These data were then corrected, pixel-by-pixel, to account for attenuation of the laser due to clear water, salt, ethanol, and dye using the methods of Daviero et al. (2001). Finally, the data were averaged to obtain the spatial distribution of average tracer concentration, and therefore dilution. The estimated accuracy of the concentration readings is $\pm 10\%$.

5. Results

Image processing techniques are useful in showing the complex three-dimensional concentration distributions.

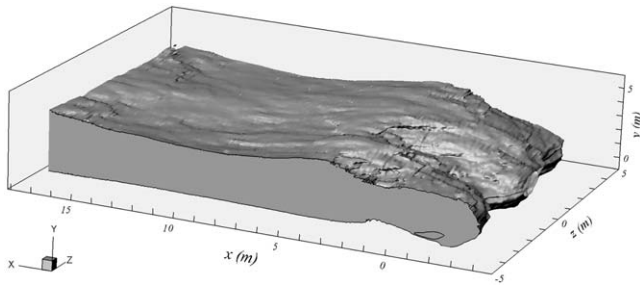


Fig. 3. Rendering of outer surface of mixing zones. Diffuser is at $x = 0$.

The outer surface of the mixing field is shown in Fig. 3. This figure was obtained by imaging an iso-concentration surface with a low threshold level. It can be seen that the upstream jets are rapidly swept downstream by the current. They then merge with those issuing in the downstream direction to form a layer about 5 m thick. The bottom of the wastefield remains essentially at the level of the ports.

The internal concentration distributions are shown in Figs. 4a,b. In these figures, the outer surface is made transparent and the concentration levels are shown as contour maps in various vertical planes that are color-coded according to the local concentration level. The levels are shown as c/c_o , i.e. they are normalized to the source concentration c_o with c the local tracer concentration. Thus the levels shown are the inverse of local dilution, S .

Variations in the longitudinal plane through the centerline of the middle riser are shown in Fig. 4a. The indi-

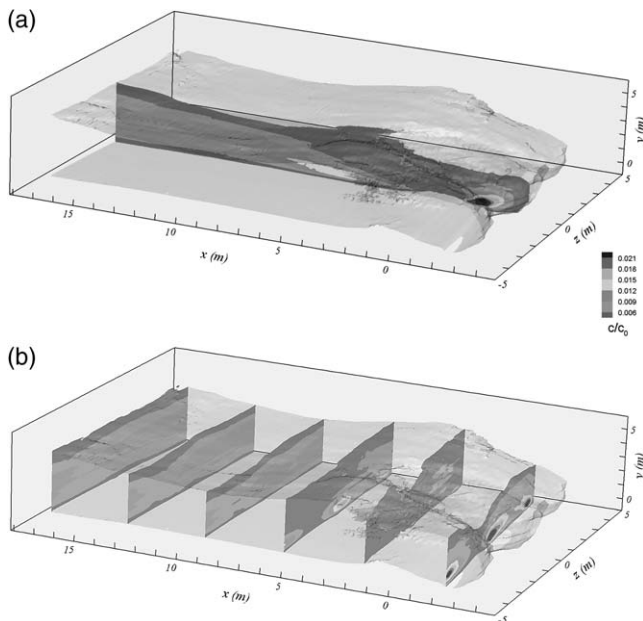


Fig. 4. Measured tracer concentration profiles in vertical planes. (a) Longitudinal plane through centerline of middle riser. (b) Lateral planes.

vidual upstream jets can be seen as areas of high concentration.

Lateral concentration variations are shown in Fig. 4b. These variations can perhaps be better seen in the three-dimensional representations shown in Fig. 5, which are in the same planes as those of Fig. 4b. Again, the upstream discharging jets can be clearly seen upstream of the diffuser by the high concentration levels in their cores. Farther downstream, at $x = 5.7$ m, the cores of the downstream discharging jets can be seen. Beyond this point, lateral mixing quickly results in the mixing layer becoming laterally homogeneous. The layer becomes essentially laterally homogeneous about 12 m downstream.

The variation of minimum dilution with distance is plotted in Fig. 6. The minimum dilution is defined as the lowest value of dilution in a vertical plane located any distance from the source. The height where this minimum dilution occurs is also plotted. It can be seen that dilution initially increases rapidly with distance from the diffuser due to intense mixing in the near field. It begins to level off when the turbulence becomes affected by ambient density stratification, and reaches a limiting value of about 113 at a distance of about 15 m; this is also where the terminal rise height is reached. Beyond this distance little further mixing occurs. In keeping with the definition of near field (see Roberts et al., 1997, and discussion), the near field dilution is therefore 113, and the length of the near field is 15 m. At the end of the near field, the mixing due to the turbulence that is generated by the discharge is suppressed by the ambient stratification.

The near field results are summarized in Table 2.

6. Comparison with mathematical models

The results were compared with the predictions of mathematical models commonly used for marine discharges and readily available from the US EPA. The models are UM3, RSB, and CORMIX. These models and their differences are described elsewhere, for example, Carvalho et al. (2001).

UM3 is a three-dimensional Lagrangian entrainment model available in the interface Visual PLUMES (Frick et al., 2001). The equations for conservation of mass, momentum, and energy are solved at each time step along the plume trajectory. The flows begin as round buoyant jets issuing from one side of the diffuser and can merge to a plane buoyant jet. The model output consists of plume characteristics along its trajectory, such as centerline dilution, width, and centerline height.

RSB is available in the Visual PLUMES interface and also as a separate Windows program RSBWIN. The model is described in Roberts (1999), where a version (called NRFIELD) that was recoded to use long time

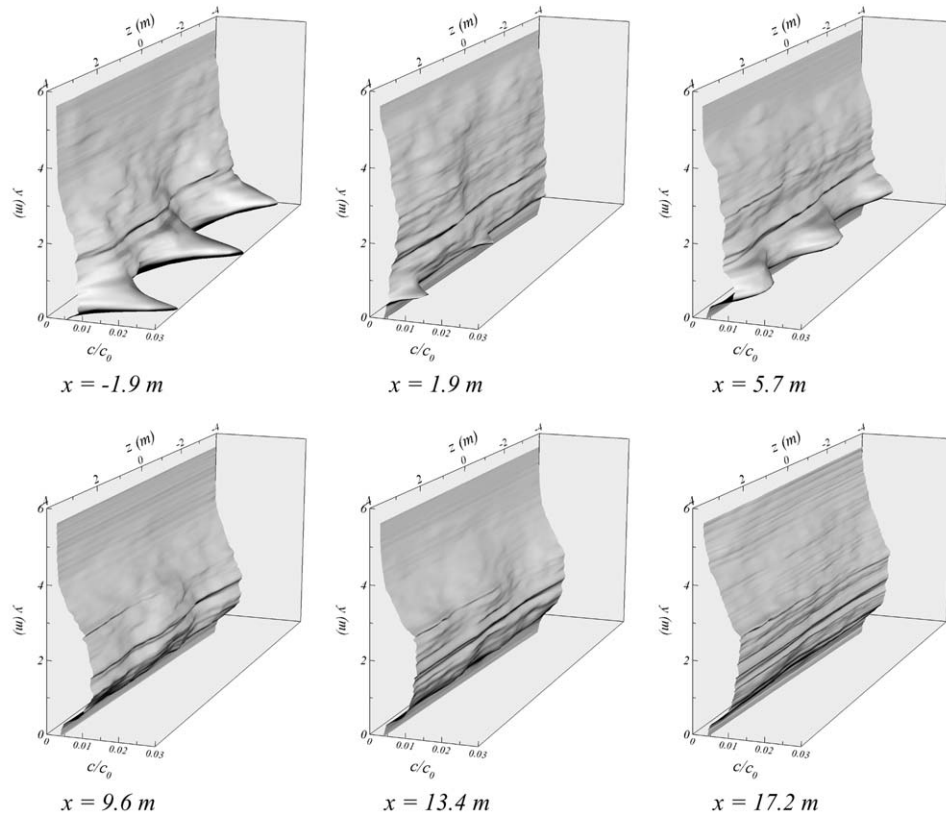


Fig. 5. Three-dimensional renderings of tracer concentration profiles in the lateral planes of Fig. 4b.

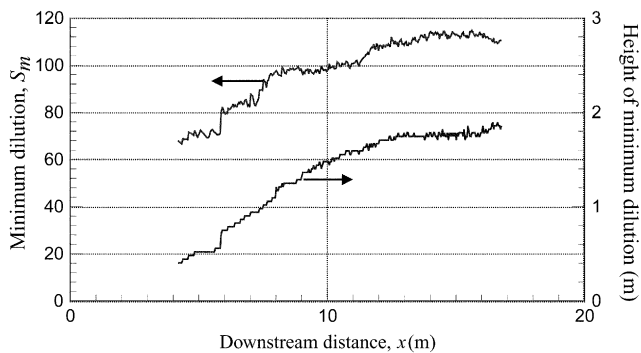


Fig. 6. Variation of minimum dilution and height of minimum dilution on diffuser centerline.

series of oceanographic data was used. RSB is based on the extensive experiments on multiport diffusers in density-stratified currents of arbitrary direction of Roberts et al. (1989). It is a length scale model that uses semi-empirical formulations based on the relative magnitudes of the dominant length scales of the problem. The model output consists of the plume characteristics (dilution, rise height, and wastefield thickness) at the end of the near field.

CORMIX (Cornell Mixing Zone Expert System) congregates several routines to analyze the geometry and dilution in the mixing zones. The subsystem CORMIX2 (Jirka and Akar, 1991) for submerged multiport diffusers was used here. CORMIX classifies the flow based on the relative magnitudes of length-scales computed from the

Table 2
Comparison of measured and predicted near field plume characteristics

Near field property	Measured	Predicted		
		RSB	UM3	CORMIX
Dilution, S_n	113	118	118	164
Length, x_n (m)	15.0	15.2	10.0	18.3
Height of dilution, z_m (m)	1.8	3.4	2.7	5.0
Wastefield thickness, h_e (m)	4.6	4.5	4.7	4.4
Height of wastefield top, z_e (m)	4.6	5.1	5.1	7.4

input information. For the cases analyzed here, CORMIX uses an eulerian entrainment model, CorJet, to obtain numerical predictions of plume behavior. Like UM3, the flows begin as round buoyant jets issuing from one side of the diffuser and can merge to a plane buoyant jet. The model output consists of plume characteristics along its trajectory, such as centerline dilution, width, and centerline height. Following termination of CorJet at the terminal rise height, or free surface, other algorithms are then used to predict further near field mixing processes, if any.

The diffuser analyzed here is typical in that the ports are opposed and discharge from both sides of the pipeline. This does not require any further assumptions in RSB, which is based on experiments with this discharge configuration (Roberts et al., 1989). Neither UM3 nor CORMIX directly accommodates this configuration, however. In UM3, the ports must all discharge in one direction. We followed the recommended approach (Frick, 2000), in which the ports are assumed to discharge horizontally from the downstream side of the diffuser with the port spacing reduced by half. This preserves the total diffuser length and the discharge per unit diffuser length. Input of the opposing port configuration into CORMIX results in the diffuser being approximated as an ‘alternating perpendicular diffuser’ in which the ports become a single row of vertically discharging round buoyant jets with equivalent total momentum flux. For the present diffuser, the net source momentum flux in any direction is zero. This is true for RSB. In UM3, the total momentum flux is directed downstream; in CORMIX, the total momentum flux is directed vertically.

The predicted properties at the end of the near field are directly outputted by RSB. The near field predictions of UM3 were assumed to be those at the maximum plume rise height, where the program terminates. Similarly, the CORMIX near field predictions were assumed to be those at the end of the CorJet module, which also occurs at the terminal rise height. Although CORMIX continues beyond this point to a ‘near field region,’ the predictions in this region were unrealistically high and were not used here.

The results are summarized in Table 2. In CORMIX, the wastefield thickness h_e was assumed to be equal to $4BV/\sqrt{2}$ where BV is the predicted Gaussian half-width of the plume.

7. Discussion

Both RSB and UM3 predict the observed dilutions closely, within experimental limits. CORMIX, however, overestimates dilution considerably, by about 45%. The length of the near field is predicted closely by RSB,

underestimated by UM3, and overestimated by CORMIX. All models reasonably predict the wastefield thickness. The height of the near field dilution is overestimated by all models, although UM3 is closest, and CORMIX overestimates it by a factor of 2.8. CORMIX also predicted that an upstream wedge of length 14.8 m would occur. This was not observed in the tests, where the jets intruded only slightly upstream due to their high source momentum flux, and were then quickly swept downstream with no upstream wedge occurring.

The main reason for the overestimation by CORMIX is probably its approximation of the discharges as vertical jets. For this diffuser, the momentum flux of the individual jets is quite high, as reflected by the relatively large value of the jet densimetric Froude number, F_j . In the actual diffuser, however, there is no net momentum flux as the momentum of the upstream jets cancels that of the downstream jets. CORMIX redirects the total momentum flux vertically, which is clearly a poor approximation in this case. UM3 directs the momentum downstream, and does not account for the upstream discharges; it can be seen that this is a good approximation for the case here. RSB is mainly intended for parameter ranges typical of ocean outfalls, in which the jet momentum is usually small. It does include the source momentum in its formulation, however, and it can be seen that it gives reliable results here.

8. Conclusions

A new three-dimensional laser induced fluorescence (3DLIF) system was applied to study the mixing of a produced water outfall discharge typical of that used in oil and gas production operations. The outfall chosen is in the Santa Barbara Channel near Carpinteria, California. It consists of a pipeline terminating in a multiport diffuser discharging into water about 12 m deep. The experimental conditions were chosen based on measured oceanographic conditions around the site. The current speed was 0.05 m/s, and the receiving water was linearly stratified. The experiments were conducted at a scale of 30.5:1, using an undistorted model based on equality of the jet densimetric Froude number. This scaling results in correct modeling of the source volume, momentum, and buoyancy fluxes, and equality of other line source dimensionless parameters. The experiments were conducted in a refractive-index-matched environment which enabled detailed three-dimensional concentration measurements in the mixing zone to be obtained.

The results showed the mixing processes to be complex. The jets discharging upstream were quickly swept downstream, where they began merging with the downstream jets. Lateral mixing caused the concentration profiles to quickly become laterally homogeneous. Initially,

dilution increased rapidly with distance from the diffuser, but farther away the rate of increase of dilution slowed as the turbulence became affected by the ambient density stratification. The dilution eventually leveled off with a value of about 113 about 15 m from the diffuser. This leveling off defines the end of the near field, in which mixing is primarily due to turbulence and processes induced by the discharge itself. At the end of the near field this turbulence collapses under the influence of the ambient stratification. The thickness of the waste-field at this point was about 5 m.

The results were compared to predictions of commonly used mathematical models of marine mixing zones: RSB, UM3, and CORMIX. The best predictions of the near field dilution and the length of the near field were by RSB. UM3 gave good predictions of the near field dilution, but CORMIX overestimated dilution and rise height substantially. CORMIX also incorrectly predicted an upstream intrusion that was not observed in the experiments. It is believed that this overestimation by CORMIX is due to its approximation of the diffuser as a row of vertically discharging jets of equivalent total momentum flux; this is clearly a poor approximation to the present situation.

3DLIF is an exciting new technique that can give unprecedented insight into the complex hydrodynamics and processes occurring in buoyancy-modified mixing zones and to improvement of near field mathematical models. Experiments on other discharge configurations are presently being conducted.

Acknowledgements

This research was funded under the STAR Program of the US Environmental Protection Agency, Exploratory Research, Physics, Grant Number R 826216. Their authors express their gratitude to the project officer, Dr. Bala Krishnan, for his assistance.

References

- Carvalho, J.L.B., Roberts, P.J.W., Roldao, J., 2001. Field observations of the Ipanema Beach outfall. *Journal of Hydraulic Engineering*, ASCE 128 (2), 151–160.
- Daviero, G.J., Roberts, P.J.W., Maile, K., 2001. Refractive index matching in large-scale stratified experiments. *Experiments in Fluids* 31, 119–126.
- Frick, W.E., Roberts, P.J.W., Davis, L.R., Keyes, J., Baumgartner, D.J., George, K.P., 2001. *Dilution Models for Effluent Discharges*, 4th edn. Visual Plumes. US Environmental Protection Agency, Environmental Research Division, NERL, Standards and Applied Science Division, Office of Science and Technology, Athens, Georgia.
- Frick, W.E., 2000. US Environmental Protection Agency, Athens, Georgia. Private communication.
- Isaacson, M.S., Koh, R.C.Y., Brooks, N.H., 1983. Plume dilution for diffusers with multiple risers. *Journal of Hydraulic Engineering*, ASCE 109 (2), 199–220.
- Jirka, G.H., Akar, P.J., 1991. Hydrodynamic classification of submerged multiport diffuser discharges. *Journal of Hydraulic Engineering*, ASCE 117 (9), 1113–1128.
- McDougall, T.J., 1979. On the elimination of refractive-index variations in turbulent density-stratified liquid flows. *Journal of Fluid Mechanics* 93 (1), 83–96.
- Roberts, P.J.W., 1979. Line plume and ocean outfall dispersion. *Journal of the Hydraulics Division*, ASCE 105 (HY4), 313–330.
- Roberts, P.J.W., Snyder, W.H., Baumgartner, D.J., 1989. Ocean outfalls, parts I, II, and III. *Journal of Hydraulic Engineering*, ASCE 115 (1), 1–70.
- Roberts, P.J.W., 1999. Modeling the Mamala Bay plumes. I: Near field. *Journal of Hydraulic Engineering*, ASCE 125 (6), 564–573.
- Roberts, P.J.W., Ferrier, A., Daviero, G., 1997. Mixing in inclined dense jets. *Journal of Hydraulic Engineering*, ASCE 123 (8), 693–699.
- Roberts, P.J.W., Snyder, W.H., 1993. Hydraulic model study for the Boston outfall. I: Riser configuration. *Journal of Hydraulic Engineering*, ASCE 119 (9), 970–987.
- Roberts, P.J.W., Tian, X., 2000. Three-dimensional imaging of stratified plume flows. In: 5th International Conference on Stratified Flows, Vancouver, British Columbia, July 10–13, 2000.
- Tian, X., Roberts, P.J.W., 2001. Application of three-dimensional imaging to plume flows. In: XXIX IAHR Congress, Beijing, China, September 16–21, 2001.
- Washburn, L., Stone, S., MacIntyre, S., 1999. Dispersion of produced water in a coastal environment and its biological implications. *Continental Shelf Research* 19, 57–78.
- Wong, D.R., Wright, S.J., 1988. Submerged turbulent buoyant jets in stagnant linearly stratified fluids. *Journal of Hydraulic Research* 26 (2), 199–223.